Fermi resonance and its effect on the mean transition time and rate

M. L. Deng and W. Q. Zhu*
Department of Mechanics, State Key Laboratory of Fluid Power Transmission and Control, Zhejiang University, Hangzhou 310027, China
(Received 13 December 2007; published 11 June 2008)

Fermi resonance and its effect on the mean transition time and rate are studied. The necessary frequency ratio 1:2 for Fermi resonance to occur is explained by applying the deterministic averaging method to the two-dimensional conservative Pippard system, and a more frequent fluctuation of energy process due to Fermi resonance is shown by using the samples obtained from digital simulation of the stochastic Pippard system. In the case of weak coupling, the mean transition time of the reacting oscillator energy is evaluated for both nonresonance and Fermi resonance by using the standard (Stratonovich) stochastic averaging method. The theoretical results for the mean transition time in the case of Fermi resonance and nonresonance is then extended to the stochastic system with bistable potential, and the effects of frequency ratio and coupling coefficient on the mean reaction rate are analyzed. In the case of strong coupling, it is pointed out that the exciting oscillator and reacting oscillator move together like one oscillator and no Fermi resonance can occur. In this case, the mean transition rate of the system total energy is studied by using the stochastic averaging method for quasi-non-integrable Hamiltonian systems. All the theoretical results are confirmed through comparison with those from digital simulation, and the effect of Fermi resonance on the transition time and rate is discussed.

DOI: 10.1103/PhysRevE.77.061114 PACS number(s): 02.50.−r, 05.10.Gg, 05.40.−a

I. INTRODUCTION

Fermi resonance gets its name from the classical work of Enrico Fermi on the Raman effect in CO_2 molecule [1]. According to Fermi's description, the three atoms in CO_2 molecule are three oscillators in one line with three natural frequencies. The ratio between two of the three natural frequencies is about 1:2. Due to the couplings between these two oscillators, there exists a specific resonant phenomenon called Fermi resonance. Fermi resonance was subsequently found in NaCl crystal [2] and, most significantly, in the protein macromolecules [3,4]. The late Mikhail Volkenstein first discussed Fermi resonance in peptide binding and indicated that it plays an important role in the functioning of an enzyme [5,6]. By establishing a two-dimensional oscillator and then introducing the coupling term x^2y to the potential, Fermi set up a simple model in 1931 [1,2]. Since then, many kinds of two-dimensional models have been set up for different research topics [3,6–11]. The physical pendulum is a classical model used by Volkenstein for analogy of Fermi resonance [3]. The dynamics of a particle bounded by four linear springs to four immobile walls was used for the investigation of Fermi resonance in a cluster model [4,7]. The energy exchange between the two coupled oscillators was proposed as a kind of promoting mechanism for the process in enzyme catalysis [8,9]. The Pippard model may be the most popular model for its pellucid physical meaning [10]. Recently, the fading of the energy between the two oscillators in Fermi resonance was investigated by performing a simulation of the Pippard model [12]. Then, as a new application, the influence of Fermi resonance on enzymatic reaction about peptide bond breaking and the escape of product from the active site were studied [12]. Many model investigations of Fermi resonance show the typical dynamical behavior that the rate of transition over a potential barrier in one oscillator increases under the effect of the other oscillator. According to this behavior, the mechanism of enzymatic reaction may be properly explained by using Fermi resonance taking place at a specific site of the enzyme, which often has the form of a "pocket." At the reaction site, the local "reactive dynamics" connected with "barrier crossing" is coupled to other oscillating degrees of freedom [11]. Note that almost all the results about Fermi resonance were obtained from computer simulation rather than theoretical method.

In the present paper, the necessary frequency ratio 1:2 for Fermi resonance is explained by applying the deterministic averaging method to a two-dimensional conservative Pippard model [10]. The typical energy fading phenomenon of Fermi resonance is observed from the samples obtained from the digital simulation of the dissipative Pippard system subjected to stochastic force. For the quasilinear Pippard system with weak coupling, the theoretical analysis of Fermi resonance is made by using the standard stochastic averaging method [13], and the mean transition time of energy in both cases of nonresonance and Fermi resonance is obtained by solving the averaged Pontryagin equation. The effects of coupling coefficient and frequency ratio on the mean transition time are discussed by using simulation results and theoretical results. The theoretical analysis is then extended to the system with two-dimensional bistable potential [11,12]. In the case of stronger coupling, the coupled exciting and reacting oscillators are treated as one oscillator and the stochastic averaging method for quasi-non-integrable Hamiltonian systems is applied to obtain the energy-controlled transition rate [14,15]. It is pointed out that no Fermi resonance can occur in the strong-coupling case. All the theoretical results are confirmed by using digital simulation.

*wqzhu@yahoo.com

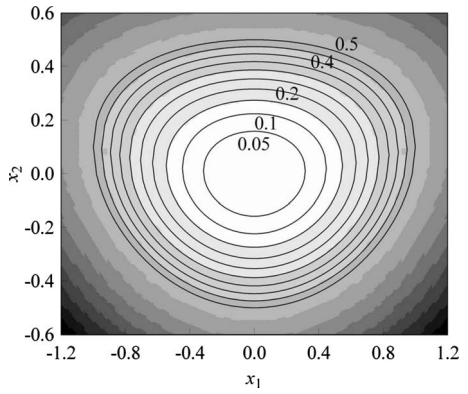

FIG. 1. Contour of Pippard potential (3) with $c=0.1$, $\omega_1=1$, and $\omega_2=2\omega_1$. The numbers in the figure are the potential values.

II. FERMI RESONANCE

The popular model for studying Fermi resonance in the peptide binding is a test particle in a two-dimensional potential $U(x_1,x_2)$ under action of noise and damping governing by the following Langevin equation [11]:

$$m\ddot{X}_1 + \gamma\dot{X}_1 + \partial U(X_1,X_2)/\partial X_1 = \sqrt{2D}\xi_1(t),$$

$$m\ddot{X}_2 + \gamma\dot{X}_2 + \partial U(X_1,X_2)/\partial X_2 = \sqrt{2D}\xi_2(t), \tag{1}$$

where X_1 is the displacement of a reacting oscillator while X_2 is the displacement of an exciting oscillator; γ is a constant damping coefficient; $\xi_1(t),\xi_2(t)$ are Gaussian white noises in the sense of Stratonovich with correlation functions

$$E[\xi_1(t)\xi_1(t+t')] = \delta(t'),$$

$$E[\xi_2(t)\xi_2(t+t')] = \delta(t'), \quad E[\xi_1(t)\xi_2(t+t')] = 0, \tag{2}$$

in which $\delta(t')$ is the Dirac delta function. In Eq. (1), the fluctuation dissipation theorem or the Einstein relation $D=\gamma k_B T$ is applied for simulating the thermal bath, where k_B is the Boltzmann constant and T is the temperature. The popular Pippard potential in the investigation of Fermi resonance is [10]

$$U(x_1,x_2) = \omega_1^2 x_1^2/2 + \omega_2^2(x_2 - cx_1^2)^2/2. \tag{3}$$

As shown in Fig. 1, potential (3) is symmetric with respect to x_1 and asymmetric with respect to x_2. For convenience of analysis, hereafter all the variables are made to be nondimensional, i.e., $m=1$, $k_B=1$, and $D=\gamma T$. By introducing potential (3) into Eq. (1), the Pippard model with two coupled oscillators reads

$$\ddot{X}_1 + \gamma\dot{X}_1 + \omega_1^2 X_1 - 2c\omega_2^2 X_1 X_2 + 2c^2\omega_2^2 X_1^3 = \sqrt{2\gamma T}\xi_1(t),$$

$$\ddot{X}_2 + \gamma\dot{X}_2 + \omega_2^2 X_2 - c\omega_2^2 X_1^2 = \sqrt{2\gamma T}\xi_2(t), \tag{4}$$

where c is usually called the coupling coefficient denoting the coupling strength between the two oscillators.

The pioneering work of Fermi on Fermi resonance is about Raman spectra of gaseous CO_2 by means of the perturbation method [1]. Fermi reported the approximate frequency ratio 1:2 (i.e., 667.5 cm^{-1} vs 1330 cm^{-1}) between two of the three natural frequencies in the CO_2 molecule and the resulting energy exchange between the two oscillators. To study Fermi resonance in the vibration of H bonds in enzyme, the ratio 1:2 was introduced to a basic two-dimensional cluster model with a particle bound by four linear springs to four immobile walls [4,7,11]. In the following, by analyzing the Pippard model system (4) in the conservative case, we explain why the frequency ratio 1:2 is necessary for Fermi resonance to occur. And then, by performing digital simulation of system (4) in the stochastic case, we show how the Fermi resonance makes the energy process different.

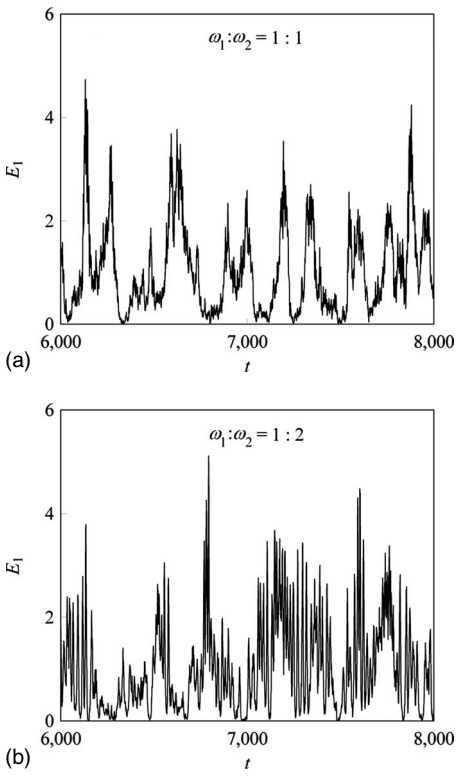

FIG. 2. Two stationary samples obtained from digital simulation of stochastic Pippard system (4) with $\gamma=0.01$, $\gamma T=0.01$, $\omega_1=1$, and $c=0.1$. More frequent energy fluctuation can be observed in the resonant case (b) than in the nonresonant case (a).

Considering the Pippard model (4) without damping and noises, and introducing the frequency ratio $\omega_1:\omega_2=n:m$, we obtain the following conservative system:

$$\ddot{x}_1 + \omega_1^2 x_1 - 2c\omega_2^2 x_1 x_2 = 0, \quad \ddot{x}_2 + \omega_2^2 x_2 - c\omega_2^2 x_1^2 = 0, \tag{5}$$

where n and m are mutual prime positive integers, and $2c^2\omega_2^2 x_1^3$ is neglected since it contains a higher order of small coupling coefficient c.

Following the well-known deterministic averaging method for quasilinear systems [16], we introduce the transformation

$$x_i = a_i(t)\cos\varphi_i(t),$$

$$\dot{x}_i = -\omega_i a_i(t)\sin\varphi_i(t), \quad \varphi_i(t) = \omega_i t + \theta_i(t), \quad i = 1,2. \tag{6}$$

The nonlinear parts of the restored force in conservative system (5) are extracted out, and then let

$$f_1(\mathbf{x},\dot{\mathbf{x}}) = -2c\omega_2^2 x_1 x_2, \quad f_2(\mathbf{x},\dot{\mathbf{x}}) = -c\omega_2^2 x_1^2, \tag{7}$$

where $\mathbf{x}=\{x_1,x_2\}$ and $\dot{\mathbf{x}}=\{\dot{x}_1,\dot{x}_2\}$. Substituting Eqs. (6) and (7) into Eq. (5) and then applying the averaging leads to the following equations for amplitudes a_1, a_2 and phase angle θ_1, θ_2:

$$da_1/dt = \langle \omega_1^{-1} f_1 \sin\varphi_1\rangle_t, \quad da_2/dt = \langle \omega_2^{-1} f_2 \sin\varphi_2\rangle_t,$$

$$d\theta_1/dt = \langle (a_1\omega_1)^{-1} f_1 \cos\varphi_1\rangle_t, \quad d\theta_2/dt = \langle (a_2\omega_2)^{-1} f_2 \cos\varphi_2\rangle_t, \tag{8}$$

where $\langle\cdot\rangle_t$ denotes time averaging. Introducing the phase angle difference $\phi=(m/n)\varphi_1-\varphi_2$ and replacing the time averaging in Eq. (8) by the phase averaging $\int_0^{2\pi}(\cdot)d\varphi_1/2\pi$, we obtain the reduced expression for da_1/dt. Moreover, according to $de_1/dt=\omega_1^2 a_1 da_1/dt$, the time rate de_1/dt for energy $e_1=\omega_1^2 a_1^2/2$ can be obtained as follows:

$$\frac{de_1}{dt} = \frac{-ce_1\sqrt{2e_2}m^2[4n\sin(m\pi)\sin(m\pi-\phi/n) + m\sin(4n\pi)\sin(\phi/n)]}{2\pi n^2(4n^2-m^2)}. \tag{9}$$

By analyzing Eq. (9), de_1/dt is reduced to

$$\frac{de_1}{dt} = \begin{cases} -2ce_1\sqrt{2e_2}\sin\phi, & n{:}m = 1{:}2, \\ 0, & n{:}m \neq 1{:}2. \end{cases} \tag{10}$$

Since $de_2/dt=-de_1/dt$, the de_2/dt and $d\phi/dt$ with $n:m=1:2$ can be obtained as follows:

$$\frac{de_2}{dt} = 2ce_1\sqrt{2e_2}\sin\phi, \quad \frac{d\phi}{dt} = \frac{\sqrt{2}c(e_1-2e_2)\cos\phi}{\sqrt{e_2}}. \tag{11}$$

It is seen from Eqs. (10) and (11) that $de_2/dt=-de_1/dt\neq 0$ only when $\omega_1:\omega_2=1:2$. In other words, the frequency ratio $\omega_1:\omega_2=1:2$ is necessary for energy exchange to occur between the two oscillators.

Digital simulation for the original system (4) was performed. The independent Gaussian white noises $\xi_i(t)$ were generated by using the Box-Muller method [17]. Then, the response was solved numerically by using the fourth-order Runge-Kutta method with time step 0.05. Two samples from digital simulation of stochastic system (4) in $\omega_1:\omega_2=1:1$ and $1:2$ are shown in Figs. 2(a) and 2(b), respectively. It is seen that in the case of Fermi resonance, energy process $E_1(t)$ fluctuates more frequently and significantly than in the nonresonant case. Similar numerical results were reported in Ref. [12], where the rather large amplitudes occur from time to time in the first oscillator.

III. MEAN TRANSITION TIME OF REACTING OSCILLATOR ENERGY

The typical phenomenon of Fermi resonance is the fading of the energy between the exciting and reacting oscillators [12]. Due to this energy fading, the random transition of the reacting oscillator over an energy threshold value happens with more probability. In the following, the mean time of transition over an energy threshold value of the reacting oscillator is predicted theoretically by using the standard stochastic averaging method [13]. Nonresonant and resonant cases are considered separately to illustrate the effect of Fermi resonance.

Let the nonlinear parts of the restored force and damping forces in system (4) be

$$F_1(\mathbf{X},\dot{\mathbf{X}}) = \gamma\dot{X}_1 - 2c\omega_2^2 X_1 X_2, \quad F_2(\mathbf{X},\dot{\mathbf{X}}) = \gamma\dot{X}_2 - c\omega_2^2 X_1^2, \tag{12}$$

where the term $2c^2\omega_2^2 X_1^3$ with higher order of small parameter c^2 is neglected. Under the assumption of $\gamma\to 0$, the solution of stochastic system (4) is assumed to be of the form

$$X_i = A_i(t)\cos\Psi_i(t),$$

$$\dot{X}_i = -\omega_i A_i(t)\sin\Psi_i(t), \quad \Psi_i(t) = \omega_i t + \Theta_i(t), \quad i = 1,2. \tag{13}$$

Here the amplitudes A_i, phase angle Ψ_i, and Θ_i are all stochastic processes. Regarding Eq. (13) as a transformation from $X_i,\dot{X}_i$ to A_i,Ψ_i, Eq. (4) can be converted into the following first-order differential equations:

$$\dot{A}_1 = F_1^A + G_{11}^A\xi_1(t), \quad \dot{\Psi}_1 = \omega_1 + F_1^\Theta + G_{11}^\Theta\xi_1(t),$$

$$\dot{A}_2 = F_2^A + G_{22}^A\xi_2(t), \quad \dot{\Psi}_2 = \omega_2 + F_2^\Theta + G_{22}^\Theta\xi_2(t), \tag{14}$$

where

$$F_1^A = F_1\sin\Psi_1/\omega_1, \quad G_{11}^A = -\sqrt{2\gamma T}\sin\Psi_1/\omega_1,$$

$$F_1^\Theta = F_1\cos\Psi_1/A_1\omega_1, \quad G_{11}^\Theta = -\sqrt{2\gamma T}\cos\Psi_1/A_1\omega_1,$$

$$F_2^A = F_2\sin\Psi_2/\omega_2, \quad G_{22}^A = -\sqrt{2\gamma T}\sin\Psi_2/\omega_2,$$

$$F_2^{\Theta} = F_2 \cos \Psi_2 / A_2 \omega_2, \quad G_{22}^{A} = -\sqrt{2\gamma T} \cos \Psi_2 / A_2 \omega_2. \tag{15}$$

In stochastic system (14), Ψ_1 and Ψ_2 are rapidly varying processes while A_1 and A_2 are slowly varying ones. The averaged equations depend upon whether system (4) is resonant or nonresonant.

A. Non-resonant case

Suppose that $\omega_1 : \omega_2$ is far from 1:2. According to the Khasminskii's theorem [18], the amplitudes A_1 and A_2 in system (14) converge in probability to a two-dimensional Markov diffusion process. The averaged Fokker-Planck-Kolmogorov (FPK) equation governing the transition probability density $p = p(\mathbf{A}, t | \mathbf{A}_0, t_0)$ is

$$\frac{\partial p}{\partial t} = -\frac{\partial}{\partial A_i}(a_i p) + \frac{1}{2}\frac{\partial^2}{\partial A_i \partial A_j}(b_{ij} p), \quad i,j = 1,2, \tag{16}$$

where $\mathbf{A} = \{A_1, A_2\}$ and the drift coefficients and diffusion coefficients are

$$a_i(\mathbf{A}) = \left\langle F_i^A + D_{kl}\frac{\partial G_{ik}^A}{\partial A_j} G_{jl}^A + D_{kl}\frac{\partial G_{ik}^A}{\partial \Theta_j} G_{jl}^{\Theta} \right\rangle_t,$$

$$b_{ij}(\mathbf{A}) = \langle 2 D_{kl} G_{ik}^A G_{jl}^A \rangle_t \quad \text{with } i,j,k,l = 1,2. \tag{17}$$

The difficult time averaging in Eq. (17) can be replaced by the following space averaging with respect to the phase angles Ψ_1 and Ψ_2:

$$\langle \cdot \rangle_t = \frac{1}{4\pi^2}\int_0^{2\pi}\int_0^{2\pi} (\cdot) d\Psi_1 d\Psi_2. \tag{18}$$

Note that $D_{11} = D_{22} = \gamma T$ and $D_{kl} = 0$ for $k \neq l$ since the two Gaussian white noises $\xi_1(t), \xi_2(t)$ are independent and of the same intensity. Substituting Eq. (15) into Eq. (17) leads to $b_{ij} = 0$ for $i \neq j$, and

$$a_1 = -\frac{\gamma A_1}{2} + \frac{\gamma T}{2A_1\omega_1^2}, \quad a_2 = -\frac{\gamma A_2}{2} + \frac{\gamma T}{8A_2\omega_1^2},$$

$$b_{11} = \frac{\gamma T}{\omega_1^2}, \quad b_{22} = \frac{\gamma T}{4\omega_1^2}. \tag{19}$$

The amplitudes A_1, A_2 and the energies E_1, E_2 of the two oscillators in system (4) are related as follows:

$$E_1 = \omega_1^2 A_1^2/2, \quad E_2 = \omega_2^2 A_2^2/2. \tag{20}$$

Thus, the drift coefficients $\bar{a}_i$ and diffusion coefficients $\bar{b}_{ii}$ of the FPK equation describing the transition probability density $p(\mathbf{E}, t | \mathbf{E}_0, t_0)$ of the energy diffusion process $\mathbf{E} = [E_1, E_2]^{\mathrm{T}}$ can be obtained by using the Itô differential rule [19] as follows:

$$\bar{a}_1 = \gamma T - \gamma E_1, \quad \bar{a}_2 = \gamma T - \gamma E_2, \quad \bar{b}_{11} = 2\gamma T E_1,$$

$$\bar{b}_{22} = 2\gamma T E_2. \tag{21}$$

In this section, we are interested in the mean time of transition over an energy threshold value of the reacting oscillator. The Pontryagin equation governing the mean transition time is [20]

$$\bar{a}_1(E_{10})\frac{\partial \tau}{\partial E_{10}} + \bar{a}_2(E_{20})\frac{\partial \tau}{\partial E_{20}} + \frac{1}{2}\bar{b}_{11}(E_{10})\frac{\partial^2 \tau}{\partial E_{10}^2} + \frac{1}{2}\bar{b}_{22}(E_{20})\frac{\partial^2 \tau}{\partial E_{20}^2} = -1, \tag{22}$$

where $\tau(E_{10}, E_{20})$ is defined as the mean time of energy process $E_1(t)$ in the reacting oscillator reaches a threshold value E_C for the first time given the initial energies $0 \leq E_{10} < E_C$, $0 \leq E_{20}$. The boundary conditions associated with Eq. (22) are

$$\tau(E_{10} = 0, E_{20}) = \text{finite}, \quad \tau(E_{10} = E_C, E_{20}) = 0, \tag{23}$$

$$\tau(E_{10}, E_{20} = 0) = \text{finite}, \quad \tau(E_{10}, E_{20} \to \infty) = \text{finite}. \tag{24}$$

Fortunately, Eq. (22) can be solved exactly under the boundary conditions (23) and (24). The exact solution is

$$\tau(E_{10}, E_{20}) = \frac{1}{\gamma}\int_{E_{10}/T}^{E_C/T} \frac{e^t - 1}{t} dt. \tag{25}$$

B. Resonant case

In the resonance domain, i.e., $\omega_1 : \omega_2 \approx 1:2$, except for the amplitudes A_1 and A_2, there exists another slowly varying process, i.e., the phase angle difference $\Phi(t) = 2\Psi_1 - \Psi_2$, which is governed by the differential equation

$$\dot{\Phi} = 0(\varepsilon) + \varepsilon F_3^A + \varepsilon^{1/2} G_{31}^A \xi_1(t) + \varepsilon^{1/2} G_{32}^A \xi_2(t), \tag{26}$$

where $F_3^A = 2F_1^{\Theta} - F_2^{\Theta}$, $G_{31}^A = 2G_{11}^{\Theta}$, and $G_{32}^A = -G_{22}^{\Theta}$; ε is a small parameter. For investigating the effect of a small deviation of the frequency ratio from $\omega_1 : \omega_2 = 1:2$, we replace the frequency ratio in Eq. (4) by $\omega_2/\omega_1 = 2 + \sigma$, where σ is a small parameter. The nonlinear parts of the restoring force and damping forces in system (4) in this case are

$$F_1(\mathbf{X}, \dot{\mathbf{X}}) = \gamma \dot{X}_1 - 2c(\omega_2^2 + 2\sigma\omega_1\omega_2) X_1 X_2,$$

$$F_2(\mathbf{X}, \dot{\mathbf{X}}) = \gamma \dot{X}_2 - c(\omega_2^2 + 2\sigma\omega_1\omega_2) X_1^2 + 2\sigma\omega_1\omega_2 X_2, \tag{27}$$

where the higher-order small terms with c^2 or σ^2 are neglected. According to Khasminskii's theorem [18], $\mathbf{A} = [A_1, A_2]^{\mathrm{T}}$ and Φ converge in probability to a three-dimensional Markov diffusion process. The FPK equation governing the transition probability density $p = p(\mathbf{A}, \Phi, t | \mathbf{A}_0, \Phi_0, t_0)$ is

$$\frac{\partial p}{\partial t} = -\frac{\partial}{\partial A_i}(a_i p) - \frac{\partial}{\partial \Phi}(a_3 p) + \frac{1}{2}\frac{\partial^2}{\partial A_i \partial A_j}(b_{ij} p) + \frac{1}{2}\frac{\partial^2}{\partial \Phi^2}(b_{33} p) + \frac{1}{2}\frac{\partial^2}{\partial A_i \partial \Phi}(b_{i3} p) + \frac{1}{2}\frac{\partial^2}{\partial \Phi \partial A_j}(b_{3j} p), \quad i,j = 1,2, \tag{28}$$

where the drift coefficients and diffusion coefficients are

$$a_i(\mathbf{A},\Phi) = \left\langle F_i^A + D_{kl}\frac{\partial G_{ik}^A}{\partial A_j}G_{jl}^A + D_{kl}\frac{\partial G_{ik}^A}{\partial \Theta_j}G_{jl}^\Theta \right\rangle_t$$
$$\text{with } i=1,2,3, \quad j,k,l=1,2,$$

$$b_{ij}(\mathbf{A},\Phi) = \langle 2D_{kl}G_{ik}^A G_{jl}^A\rangle_t \quad \text{with } i,j=1,2,3, \quad k,l=1,2. \tag{29}$$

Again, the time averaging can be replaced by the following space averaging with respect to the phase angle Ψ_1:

$$\langle\cdot\rangle_t = \frac{1}{2\pi}\int_0^{2\pi}(\cdot)d\Psi_1. \tag{30}$$

Note that $D_{11}=D_{22}=\gamma T$ and $D_{kl}=0$ for $k\neq l$. Substituting Eqs. (15) and (26) into Eq. (29) leads to $b_{ij}=0$ for $i\neq j$. The other coefficients are reduced to

$$a_1 = -\frac{\gamma A_1}{2} + \frac{\gamma T}{2A_1\omega_1^2} - 2c(1+\sigma)A_1A_2\omega_1\sin\Phi,$$

$$a_2 = -\frac{\gamma A_2}{2} + \frac{\gamma T}{8A_2\omega_1^2} + \frac{1}{2}c(1+\sigma)A_1^2\omega_1\sin\Phi,$$

$$a_3 = -\sigma\omega_1 + \frac{c(1+\sigma)\omega_1(A_1^2-8A_2^2)\cos\Phi}{2A_2},$$

$$b_{11} = \frac{\gamma T}{\omega_1^2}, \quad b_{22} = \frac{\gamma T}{4\omega_1^2}, \quad b_{33} = \frac{4\gamma T}{A_1^2\omega_1^2} + \frac{\gamma T}{4A_2^2\omega_1^2}. \tag{31}$$

The FPK equation describing the transition probability density $p(\mathbf{E},\Phi,t|\mathbf{E}_0,\Phi_0,t_0)$ of diffusion process $[E_1,E_2,\Phi]^T$ can also be set up by using relation (20), and its drift coefficients $\bar{a}_i$ and diffusion coefficients $\bar{b}_{ii}$ are obtained from Eq. (31) by using the Itô differential rule [19] as follows:

$$\bar{a}_1 = \gamma T - \gamma E_1 - 2c(1+\sigma)E_1\sqrt{2E_2}\sin\Phi,$$

$$\bar{a}_2 = \gamma T - \gamma E_2 + 2c(1+\sigma)E_1\sqrt{2E_2}\sin\Phi,$$

$$\bar{b}_{11} = 2\gamma T E_1, \quad \bar{b}_{22} = 2\gamma T E_2. \tag{32}$$

Define τ as the mean time of energy process $E_1(t)$ in the reacting oscillator reaches a threshold value E_C for the first time given the initial energy $0\le E_{10}<E_C$, $0\le E_{20}$, and initial phase angle difference Φ_0. The Pontryagin equation governing τ can be derived from Eq. (28) as follows [20]:

$$\bar{a}_1\frac{\partial\tau}{\partial E_{10}} + \bar{a}_2\frac{\partial\tau}{\partial E_{20}} + a_3\frac{\partial\tau}{\partial\Phi_0} + \frac{1}{2}\bar{b}_{11}\frac{\partial^2\tau}{\partial E_{10}^2} + \frac{1}{2}\bar{b}_{22}\frac{\partial^2\tau}{\partial E_{20}^2} + \frac{1}{2}b_{33}\frac{\partial^2\tau}{\partial\Phi_0^2} = -1. \tag{33}$$

The boundary conditions associated with Eq. (33) are

$$\tau(E_{10}=0,E_{20},\Phi_0)=\text{finite}, \quad \tau(E_{10}=E_C,E_{20},\Phi_0)=0, \tag{34}$$

$$\tau(E_{10},E_{20}=0,\Phi_0)=\text{finite}, \quad \tau(E_{10},E_{20}\to\infty,\Phi_0)=\text{finite}, \tag{35}$$

$$\tau(E_{10},E_{20},\Phi_0=2\pi)=\tau(E_{10},E_{20},\Phi_0=0). \tag{36}$$

It is difficult to obtain the exact analytical solution to Eq. (33). For convenience to obtain numerical solution, the second boundary condition at infinite in Eq. (35) is converted to the following boundary condition at some finite place using the transformation $\bar{E}_{20}=1-\exp(-E_{20})$:

$$\tau(E_{10},\bar{E}_{20}=0,\Phi_0)=\text{finite}, \quad \tau(E_{10},\bar{E}_{20}=1,\Phi_0)=\text{finite}. \tag{37}$$

The Pontryagin equation (33) should be correspondingly changed to

$$\bar{a}_1\frac{\partial\tau}{\partial E_{10}} + \bar{\bar{a}}_2\frac{\partial\tau}{\partial\bar{E}_{20}} + a_3\frac{\partial\tau}{\partial\Phi_0} + \frac{1}{2}\bar{b}_{11}\frac{\partial^2\tau}{\partial E_{10}^2} + \frac{1}{2}\bar{\bar{b}}_{22}\frac{\partial^2\tau}{\partial\bar{E}_{20}^2} + \frac{1}{2}b_{33}\frac{\partial^2\tau}{\partial\Phi_0^2} = -1, \tag{38}$$

where the two new coefficients $\bar{\bar{a}}_2(E_{10},\bar{E}_{20},\Phi_0)$ and $\bar{\bar{b}}_{22}(E_{10},\bar{E}_{20},\Phi_0)$ are obtained from $\bar{a}_2$ and $\bar{b}_{22}$ in Eq. (32) by using the Itô differential rule [19] as follows:

$$\bar{\bar{a}}_2 = \bar{a}_2\frac{d}{dE_2}(1-e^{-E_2}) + \frac{1}{2}\bar{b}_{22}\frac{d^2}{dE_2^2}(1-e^{-E_2}),$$

$$\bar{\bar{b}}_{22} = \left[\frac{d}{dE_2}(1-e^{-E_2})\right]^2\bar{b}_{22}. \tag{39}$$

Some numerical results shown in Fig. 3 are obtained from solving Eq. (38) together with boundary conditions (34), (36), and (37). The number in the figures is the value of the mean transition time τ. Figure 3 shows that the mean time of the transition of the reacting oscillator over an energy threshold value decreases as initial energy E_{10} of the reacting oscillator or $\bar{E}_{20}$ of the exciting oscillator increases. With regard to the initial phase angle difference Φ_0, the mean transition time is minimum at $\Phi_0=3\pi/2$ and maximum at $\Phi_0=\pi/2$ when E_{10} and $\bar{E}_{20}$ are kept unchanged. It can be seen from Eq. (32) that when $\gamma=0$, $\bar{a}_1$ reaches its maximum at $\Phi_0=3\pi/2$, which means the rate of input energy, dE_1/dt, in reacting oscillator reaches its maximum. As a result, the mean time τ of transition of the reacting oscillator over an energy threshold value E_C reduces to its minimum. The mean time τ reaching its maximum at $\Phi_0=\pi/2$ can be explained similarly. To check the accuracy of the theoretical result shown in Fig. 3, the digital simulation of original system (4) was conducted. For each sample, the time of transition of $E_1(t)$ over an energy threshold value E_C is recorded. For given E_{10}, $\bar{E}_{20}$, and Φ_0, the mean time is then obtained from averaging the transition times for 2000 samples. Figure 4 shows some simulation results for the same parameters as those in Fig. 3. It is seen that good agreement between the

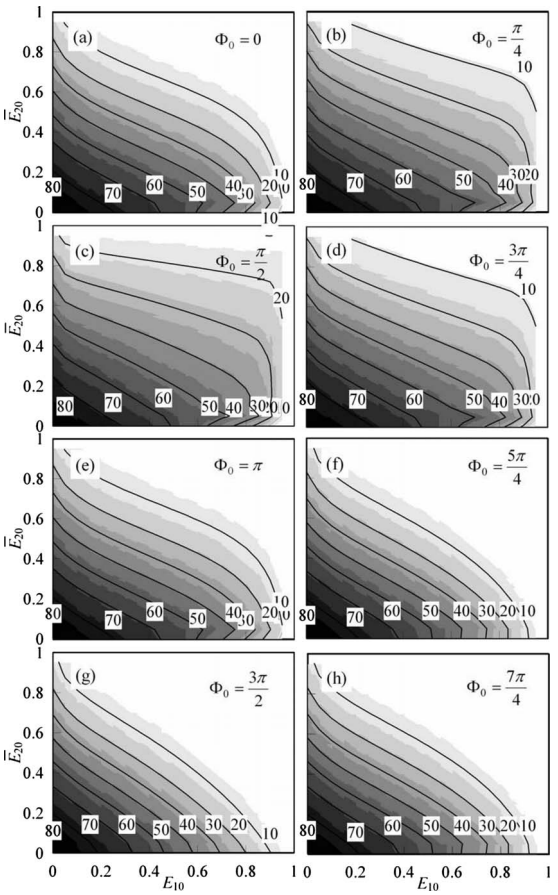

FIG. 3. Mean transition time τ as functions of initial energy E_{10}, $\bar{E}_{20}$, and initial phase angle Φ_0 obtained from solving Eq. (38). The parameters are $c=0.1$, $\sigma=0$, $\gamma=0.01$, $\gamma T=0.01$, $E_C=1$, $\omega_1=1$, and $\omega_2=2\omega_1$. The numbers in the figures are the mean time τ, which is symmetric with respect to $\Phi_0=\pi/2$ and $3\pi/2$ and reaches its maximum and minimum at $\Phi_0=\pi/2$ and $3\pi/2$, respectively.

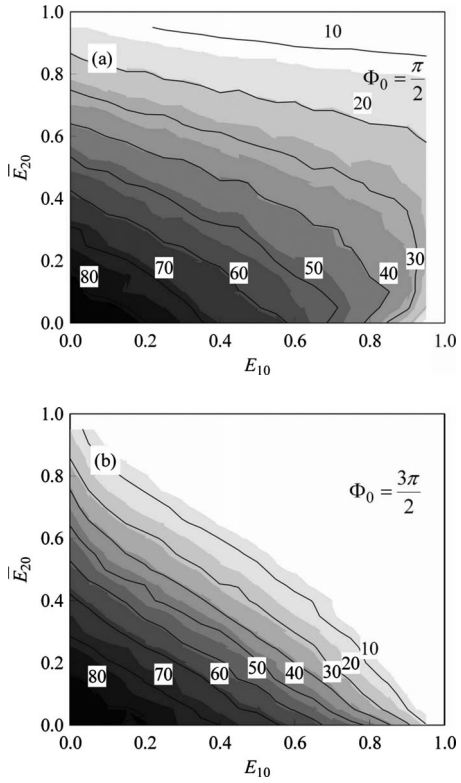

FIG. 4. Mean transition time τ as functions of initial energy E_{10}, $\bar{E}_{20}$, and initial phase angle Φ_0 obtained from digital simulation of system (4) with the same parameters as those in Fig. 3. The simulation results in (a) and (b) fit well the theoretical results shown in Figs. 3(c) and 3(g), respectively.

theoretical results in Figs. 3(c) and 3(g) and corresponding simulation results in Figs. 4(a) and 4(b), respectively, is achieved.

In the resonant case, coupling coefficient c plays an important role in energy exchange between reacting oscillator and exciting oscillator. Figure 5 shows how the mean transition time τ varies with c for two E_C values. It is seen that the mean transition time τ increases as E_C increases, while it decreases as the coupling coefficient c increases. This implies that Fermi resonance really enhances the transition of the reacting oscillator. However, it should be pointed out that as c gradually increases, the theoretical results become doubtful since the stochastic averaging is based on the assumption of weak coupling between reacting oscillator and exciting oscillator. The mean transition time τ for frequency ω_2 varying from $10^{-2}\omega_1$ to $10^2\omega_1$ is shown in Fig. 6. The long dashed line (−−) and solid line (——) denote the theoretical results in the case of nonresonance, which are obtained from Eq. (25). The short dashed line (------) and dash-dotted line (−·−) denote the theoretical results in the case of resonance, which are obtained by solving Eq. (38). The symbols • and ◆ denote the corresponding digital simulation results. It is seen that τ reaches its minimum at Fermi resonance frequency $\omega_2=2\omega_1$. Comparing with the nonresonant case, it is shown that Fermi resonance can reduce the mean transition time by about 62.1% for theoretical results and 64.8% for simulation results when $E_C=1$, and about 54.1% for theoretical results and 53.2% for simulation results when $E_C=2$. The agreement between the theoretical results and the digital simulation results illustrates the applicable ranges of the exact solution in Eq. (25) for the nonresonant case and

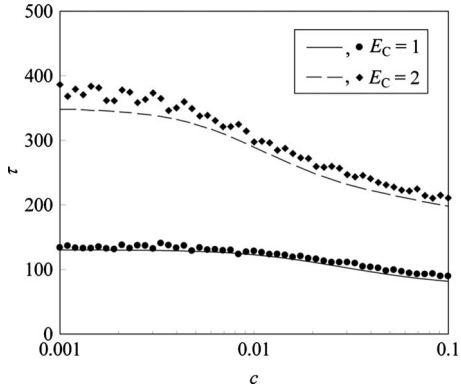

FIG. 5. Mean transition time τ of system (4) as a function of coupling coefficient c. The parameters are $\sigma=0$, $\gamma=0.01$, $\gamma T=0.01$, $\omega_1=1$, and $\omega_2=2\omega_1$. The solid and dashed lines denote the theoretical results, and symbols •, ◆ denote the corresponding simulation results.

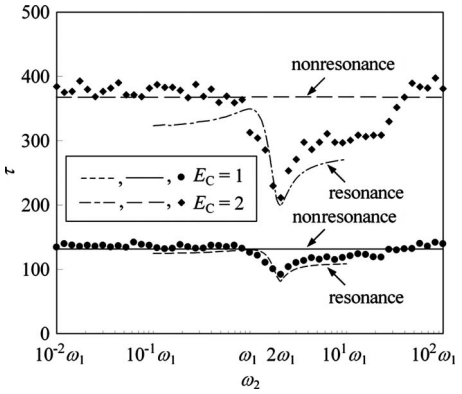

FIG. 6. Mean transition time τ as a function of frequency ω_2. The theoretical results for the nonresonant case are obtained from Eq. (25) while those for the resonant case are obtained from solving Eq. (38). $c=0.1$ and the other parameters are the same as those in Fig. 5.

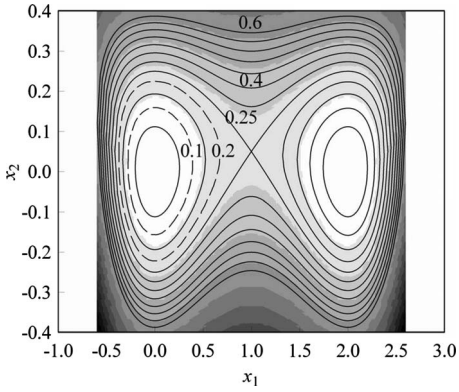

FIG. 7. Contour of potential (45) with $a=1$, $b=1$, $\alpha=4a$, and $c=0.2$. The numbers in the figure are the potential values and the dashed line denotes the energy threshold value E_C used in Sec. V.

the numerical solution to Eq. (38) for the resonant case. For predicting the mean transition time τ in a large frequency range of ω_2 varying from $10^{-2}\omega_1$ to $10^{2}\omega_1$, it is necessary to use Eqs. (25) and (38) alternatively in the nonresonant case or the resonant case.

IV. EXTENSION TO A SYSTEM WITH BISTABLE POTENTIAL

The classical Kramers reaction rate theory is based on a model describing a test particle moving in a double-well potential,

$$U_0(x_1) = ax^2 - \sqrt{ab}x_1^3 + bx_1^4/4. \tag{40}$$

Two relevant frequencies are $\omega_0=\sqrt{2a}$ defined at the potential well bottom where the transition starts and $\omega_b=\sqrt{a}$ at the potential well top where the transition happens. The potential barrier height is

$$\Delta U = a^2/4b. \tag{41}$$

The classical Kramers reaction rate theory regards the reaction as a reacting particle transition over a potential barrier due to stochastic fluctuation and yields the reaction rate (transition rate)

$$k_M = \left[\left(\frac{\gamma^2}{4} + \omega_b^2\right)^{1/2} - \frac{\gamma}{2}\right]\frac{\omega_0}{2\pi\omega_b}\exp\left(\frac{-\Delta U}{k_B T}\right) \tag{42}$$

for moderate and large damping γ regime, and

$$k_W = \frac{\gamma\Delta U}{k_B T}\exp\left(\frac{-\Delta U}{k_B T}\right) \tag{43}$$

for weak damping. Combining the two reaction rates, Kramers arrived at an estimation for the general reaction rate [21],

$$k = (k_M^{-1} + k_W^{-1})^{-1}, \tag{44}$$

which is applicable in all damping regimes.

In this section, we study the enhancement of the reaction rate due to Fermi resonance in a system with a double-well potential. For this purpose, we use the following two-dimensional bistable potential model proposed by Ebeling [11]:

$$U(x_1,x_2) = U_0(x_1) + \alpha[x_2 - cU_0(x_1)]^2. \tag{45}$$

As shown in Fig. 7, potential (45) is symmetric with respect to x_1 and asymmetric with respect to x_2. By substituting Eq. (45) into Eq. (1), a system with a double-well potential and coupling between the reacting oscillator and exciting oscillator is obtained. The linear frequencies of the two oscillators at the potential well bottom are $\omega_{10}=\sqrt{2a}$ and $\omega_{20}=\sqrt{2\alpha}$, respectively, and $\alpha=4a$ corresponds to $\omega_1:\omega_2=1:2$. Fermi resonance would occur when a reacting particle is moving in the domain near the potential well bottom (see Fig. 7). Actually, the Kramers reaction rate (43) can be obtained by using the stochastic averaging method for quasi-Hamiltonian systems via linear approximation $U_0(x_1)\approx ax_1^2$ and high potential barrier approximation $\Delta U/k_B T \gg 1$ [22]. In this section, we are going to find the applicability and precision of the theoretical results in Sec. III in determining the reaction rate of system (1) with potential (45). Here the linear approximation is again used. Replacing ω_1 and c with $\sqrt{2a}$ and ca in Eqs. (31) and (32) and replacing E_C with ΔU in boundary condition (34), the mean transition time τ of the reacting oscillator over potential barrier ΔU in the Fermi resonance case can be predicted theoretically by solving the Pontryagin equation (38) associated with boundary conditions (34), (36), and (37). Hereafter, the mean transition time τ exactly means the mean time $\tau(E_{10},\bar{E}_{20},\Phi_0)$ at $E_{10}=0$, $\bar{E}_{20}=0$, and $\Phi_0=0$. The mean time τ in the nonresonant case can be obtained from Eq. (25). The reaction rate k is then obtained as the inverse of the mean transition time τ, i.e., $k=1/\tau$ [23].

Some numerical results obtained from the solution to Eq. (38), and digital simulation, as well as Kramers' formula (44) are shown in Fig. 8. The solid line (——), long dashed line (– –), and short dashed line (------) denote the theoretical results obtained by solving Eq. (38) with coupling coefficient $c=0$, 0.1, and 0.2, respectively. The symbols •, ◆, and ■ denote the corresponding digital simulation results. The dash-dotted line (–·–) denotes the theoretical results obtained from Kramers' formula (44). Good agreement be-

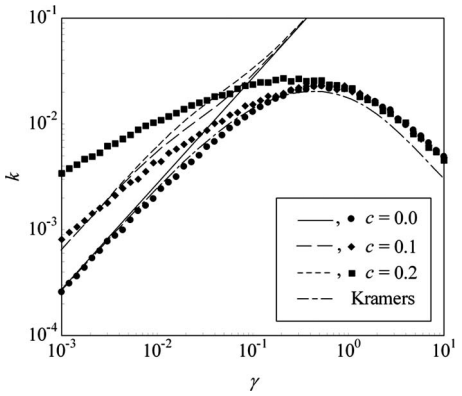

FIG. 8. The reaction rate k of system (1) with potential (45) for potential barrier $\Delta U=2k_BT$. The linear frequency ratio is $\omega_1:\omega_2=1:2$ and the other parameters are the same as those in Fig. 7. The lines denote the theoretical results and symbols denote the corresponding simulation results.

tween theoretical results and simulation results is achieved in the case of weak damping and weak coupling. When coupling coefficient $c=0$, i.e., no coupling between the two oscillators, the theoretical result exactly reduces to the Kramers result. When $c>0$, the Fermi resonance leads to an increasing of reaction rate due to the energy exchange between the reacting oscillator and exciting oscillator. For $0\leq c<0.1$ and $\gamma<0.01$, the theoretical method used in this paper can yield satisfactory prediction for the reaction rate of the reacting oscillator over the potential barrier in both the nonresonant and resonant cases. With α varying from $10^{-2}a$ to $20a$, the value of reaction rate k is shown in Fig. 9. The long dashed line (– –) and solid line (——) denote the theoretical results in the case of nonresonance, which are obtained from Eq. (25). The short dashed line (------) and dash-dotted line (–·–) denote the theoretical results in the case of resonance, which are obtained by solving Eq. (38). The symbols • and ♦ denote the corresponding digital simulation results. It can be seen that k reaches its maximum at $\alpha=4a$ corresponding to the linear frequency ratio $\omega_1:\omega_2=1:2$. Comparing with

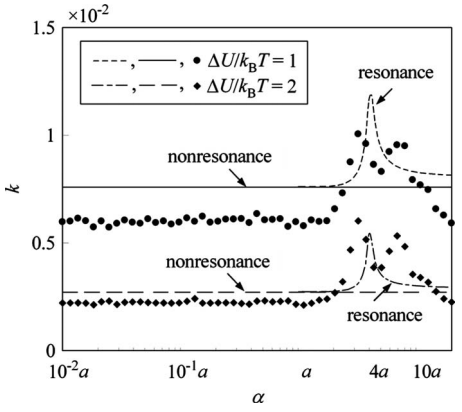

FIG. 9. The reaction rate k of system (1) with potential (45) as a function of α. $c=0.1$ and the other parameters are the same as those in Fig. 8. The theoretical results for the nonresonant case are obtained from Eq. (25) and those for the resonant case are obtained by solving Eq. (38).

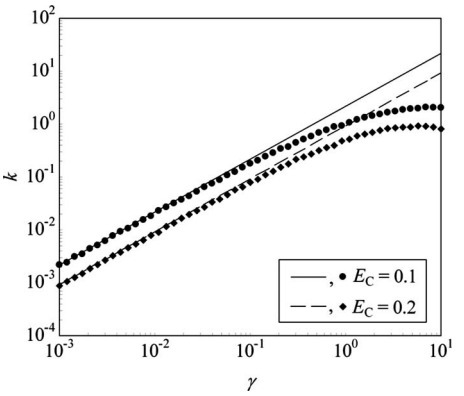

FIG. 10. The transition rate k of the total energy of system (1) with potential (45) with strong coupling for threshold value E_C. $c=1$, $a=1$, $b=1$, $\alpha=4a$, and $\Delta U/k_BT=2$.

the nonresonant case, it is shown that Fermi resonance can enhance reaction rate by about 156% for theoretical results (176% for simulation results) when $\Delta U/k_BT=1$, and about 201% for theoretical results (285% for simulation results) when $\Delta U/k_BT=2$. For predicting the reaction rate k in a large range of α varying from $10^{-2}a$ to $20a$, it is necessary to use Eqs. (25) and (38) alternatively for the nonresonant and resonant cases. Comparing with Fig. 6, a greater difference between the theoretical result and the simulation result can be observed in Fig. 9 due to the linear approximation $U_0(x_1)\approx ax_1^2$.

V. TRANSITION RATE OF TOTAL ENERGY IN THE CASE OF STRONG COUPLING

The theoretical results obtained in Secs. III and IV are based on the assumption of weak coupling. In the case of strong coupling, the reacting oscillator and the exciting oscillator in Eq. (1) will move together as one oscillator rather than separately and the system can be regarded as a quasi-non-integrable Hamiltonian system. In this case, it is more reasonable to consider the dynamical behavior of the following Hamiltonian H (the system total energy):

$$H=v_1^2/2+v_2^2/2+U(x_1,x_2), \tag{46}$$

where the potential $U(x_1,x_2)$ has been defined in Eq. (45). As reported in Ref. [22], the stochastic averaging method for a quasi-non-integrable Hamiltonian system [24] yields the following mean time for Hamiltonian process $H(t)$ reaching a threshold value E_C for the first time given initial Hamiltonian $H_0<E_C$:

$$\tau(H_0)=2\int_{H_0}^{E_C}du\int_0^u\frac{1}{\sigma^2(v)}\exp\left[-2\int_v^u\frac{m(w)}{\sigma^2(w)}dw\right]dv, \tag{47}$$

where the drift coefficient $m(H)$ and diffusion coefficient $\sigma^2(H)$ read

$$m(H)=2\gamma k_BT-2\gamma H+2\gamma G(H),$$

$$\sigma^2(H)=4\gamma k_BTH-4\gamma k_BTG(H),$$

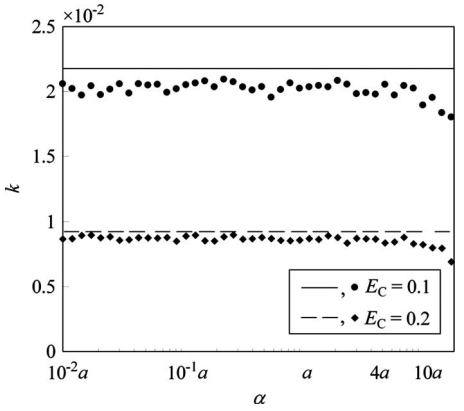

FIG. 11. The transition rate k of the total energy of system (1) with potential (45) in the strong-coupling case for threshold value E_C as function of parameter α. γ=0.01 and the other parameters are the same as those in Fig. 10.

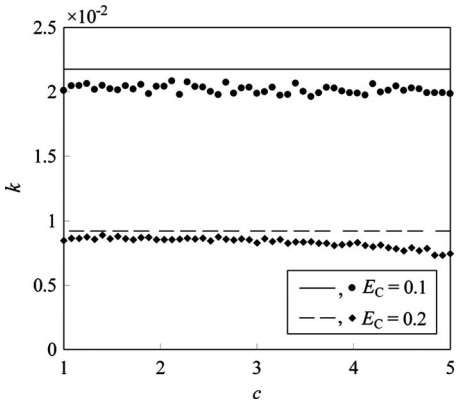

FIG. 12. The transition rate k of the total energy of system (1) with potential (45) in the strong-coupling case for threshold value E_C as a function of coupling coefficient c. γ=0.01 and the other parameters are the same as those in Fig. 10.

$$G(H) = \iint_{\Sigma} U(x_1,x_2)dx_1dx_2 \Big/ \iint_{\Sigma} dx_1dx_2,$$

$$\Sigma = \{(x_1,x_2)|U(x_1,x_2) \leq H\}. \tag{48}$$

Note that the theoretical result (47) is applicable for all kinds of potential $U(x_1,x_2)$. Here, the potential (45) is employed.

In Figs. 10–12, some theoretical results for $\tau(H_0=0)$ and corresponding simulation results are shown to illustrate the validity of the theoretical method and the effects of parameters E_C, α, and c on transition rate k. It is seen from Fig. 10 that the transition rate k decreases as the threshold value E_C increases and the theoretical results are useful in the weak damping case. It is seen from Fig. 11 that the transition rate of system total energy does not change much at resonant frequency $\alpha=4a$. Figure 12 shows that the coupling coefficient c has no remarkable influence on the transition rate of system total energy provided c is larger than 1.

VI. CONCLUSIONS

In the present paper, the deterministic averaging method has been used to explain the necessary frequency ratio 1:2 for Fermi resonance to occur in coupled exciting and reacting oscillators. Two stationary samples have been obtained from digital simulation to show more frequent and more significant fluctuation in energy process due to Fermi resonance. The standard stochastic averaging method has been used to study the Fermi resonance between the exciting oscillator and reacting oscillator in the case of weak damping and weak coupling. Through solving the Pontryagin equation for an averaged system, the mean transition time of the reacting oscillator over an energy threshold value E_C has been obtained for both resonant and nonresonant cases. The obtained results are then verified by comparing with the results obtained from digital simulation. It has been shown that the mean transition time $\tau(E_{10},\bar{E}_{20},\Phi_0)$ in the case of Fermi resonance decreases as initial energies of E_{10} or $\bar{E}_{20}$ increase. The mean transition time reaches maximum and minimum, respectively, at initial phase angle difference $\Phi_0=\pi/2$ and $3\pi/2$. As the energy threshold value E_C increases, the mean transition time increases correspondingly. While the coupling coefficient c increases, the mean transition time decreases. By observing a broad range of frequency ratio, it was found that the mean transition time in the resonant case is remarkably lower than that in the nonresonant domain, which implies that the Fermi resonance leads to an increase of the transition rate due to the energy exchange between exciting oscillator and reacting oscillator. As a further investigation, the Fermi resonance in a two-dimensional system with a bistable potential has been studied. Under the linear approximation $U_0(x_1)\approx ax_1^2$, the transition rates in a reacting oscillator in both the resonant and nonresonant cases have been predicted. When there is no coupling between the exciting and reacting oscillators, the theoretical result is the same as Kramer's result for weak damping. In the case of strong coupling, the system should be regarded as a quasi-non-integrable Hamiltonian system and no Fermi resonance can occur. In this case, the transition rate of system total energy H over an energy threshold value E_C has been obtained by solving a Pontryagin equation after applying the stochastic averaging method for quasi-non-integrable Hamiltonian systems. Finally, good agreement between theoretical results and simulation results has been achieved.

ACKNOWLEDGMENTS

The work reported in this paper was supported by the National Natural Science Foundation of China under Grants No. 10332030 and No. 10772159 and the Research Fund for the Doctoral Program of Higher Education of China under Grant No. 20060335125.

[1] E. Fermi, Z. Phys. **71**, 250 (1931).
[2] E. Fermi and F. Rasetti, Z. Phys. **71**, 689 (1931).
[3] M. V. Volkenstein, Izd. Akad. Nauk., Moscow (1947) (in Russian).
[4] E. Shidlovskaya, L. Schimansky-Geier, and Yu. M. Romanovsky, Z. Phys. Chem. **214**, 65 (2000).
[5] M. V. Volkenstein, *Molecular Biophysics* (Academic, New York, 1977).
[6] M. V. Volkenstein, I. B. Golovanov, and V. M. Sobolev, *Molecular Orbitals in Enzymology* (Nauka, Moscow, 1982) (in Russian).
[7] A. Netrebko, N. Netrebko, Yu. M. Romanovsky, Yu. Khurgin, and E. Shidlovskaya, Izv. Vuzov: Prikladnaya Nelineinaya Dinamika **2**, 26 (1994) (in Russian).
[8] W. Ebeling, Biomed. Biochim. Acta **44**, 831 (1985).
[9] W. Ebeling and Yu. M. Romanovsky, Z. Phys. Chem. (Leipzig) **266**, 836 (1985).
[10] A. B. Pippard, *The Physics of Vibration: The Simple Vibrator in Quantum Mechanics* (Cambridge University Press, Cambridge, 1983).
[11] W. Ebeling, L. Schimansky-Geier, and Yu. M. Romanovsky, *Stochastic Dynamics of Reacting Biomolecules* (World Scientific, Singapore, 2003).
[12] W. Ebeling, A. Kargovsky, A. Netrebko, and Yu. M. Romanovsky, Fluct. Noise Lett. **4**, L183 (2004).
[13] R. L. Stratonovich, *Topics in the Theory of Random Noise* (Gordon and Breach, New York, 1963), Vol. 1.
[14] W. Q. Zhu, ASME Applied Mechanics Reviews **59**, 230 (2006).
[15] W. Q. Zhu, *Nonlinear Stochastic Dynamics and Control—A Hamiltonian Theoretical Framework* (Science Press, Beijing, 2003) (in Chinese).
[16] N. N. Bogolyubov and Yu. A. Mitroplskii, *Asymptotic Methods in Nonlinear Vibration Theory* (Nauka, Moscow, 1974) (in Russian).
[17] G. Box and M. Muller, Ann. Math. Stat. **29**, 610 (1958).
[18] R. Z. Khasminskii, Izv. Akad. Nauk SSSR, Tekh. Kibern. **4**, 260 (1968) (in Russian).
[19] K. Itô, Mem. Am. Math. Soc. **4**, 289 (1951).
[20] L. S. Pontryagin, A. A. Andronov, and A. A. Vitt, Zh. Eksp. Teor. Fiz. **3**, 165 (1933) (in Russian).
[21] P. Hänggi, P. Talkner, and M. Borkovec, Rev. Mod. Phys. **62**, 251 (1990).
[22] M. L. Deng and W. Q. Zhu, Chin. Phys. **16**, 1510 (2007).
[23] P. Reimann, G. J. Schmid, and P. Hänggi, Phys. Rev. E **60**, R1 (1999).
[24] W. Q. Zhu and Y. Q. Yang, Trans. ASME, J. Appl. Mech. **64**, 157 (1997).